

## DEVELOPMENT OF A TEST BENCH FOR CATALYTIC ELECTROTHERMAL THRUSTERS

José Albuquerque Junior, [jose@lcp.inpe.br](mailto:jose@lcp.inpe.br)  
Ricardo Amaral Contaifer, [contaifer@lcp.inpe.br](mailto:contaifer@lcp.inpe.br)  
Turíbio Gomes Soares Neto, [turibio@lcp.inpe.br](mailto:turibio@lcp.inpe.br)  
Fernando de Souza Costa, [fernando@lcp.inpe.br](mailto:fernando@lcp.inpe.br)

Laboratório Associado de Combustão e Propulsão  
Instituto Nacional de Pesquisas Espaciais  
Rodovia Presidente Dutra, km 40, Cachoeira Paulista, SP, 12630-000, Brasil

**Abstract.** Catalytic resistojets are small thrusters that use electric power and a catalyst to heat and decompose a propellant before exhaustion through a nozzle. This paper describes the design and construction of a bench for testing electrothermal catalytic thrusters, and the design, construction and tests of a 0.2 N thruster using self-pressurized nitrous oxide ( $N_2O$ ) as propellant. The systems for fuel storage, ducting, injection, heating, exhaustion, instrumentation and data acquisition are described. Preliminary tests with no propellant decomposition and power input from 100 to 400 W have reached specific impulses from 70 to 120 s with thrust levels from 150 to 250 mN. The  $N_2O$  decomposition was achieved by a pre-heated  $Ru/Al_2O_3$  catalyst.

**Keywords:** resistojet, test bench, catalyst, heater, thruster, performance

### 1. INTRODUCTION

Catalytic resistojets are electrothermal thrusters with low thrust ( $\sim 1N$ ) which use a heater and a catalytic bed to heat and decompose the propellant before its ejection by a nozzle. They can be used, for example, in orbit correction, positioning and attitude maintenance of satellites (Hoole, 1990).

The addition of electric energy allows a better use of propellant, and can increase the lifetime of satellites and probes, the reach of space missions or to reduce the launching costs (Szabo et al, 1995). The first use of a resistojet in space was in the 1960s, in the Vela satellite built by TRW Systems to detect nuclear explosions (Jahn, 1968).

Electric propulsion systems can present a payload ratio, or mass efficiency, greater than chemical propulsion systems, if the power supply system mass is not large. A higher mass efficiency is obtained when the heating power used is available on shared with other equipments on board, when they are turned off or have reduced their power demand (Sutton, 1992).

Although the thrust values are, in general, small compared to other types of propulsive systems, electric thrusters yield greater propellant exhaustion velocities and, consequently, larger specific impulses. The low thrusts allow maneuvers of high precision, required to observe fixed points on Earth surface or on other celestial bodies (Giacobone, 2003).

Resistojets are the simplest electric thrusters, being able to use different propellants such  $H_2$ ,  $N_2$ ,  $CO$ ,  $CO_2$ ,  $H_2O$ ,  $He$ ,  $H_2O$ ,  $Xe$ ,  $NH_3$  and  $N_2H_4$ . They are easy to control, have a simple power conditioning system, allow the use of inert propellants, are reliable, present low cost and have a good thrust efficiency, from 60 to 85% (Sutton, 1992).

The specific impulse,  $I_{sp}$ , is the ratio of thrust and propellant weight consumption rate. Resistojets have, in general,  $I_{sp}$  lower ( $< 300$  s) than other electric thrusters, however provide relatively higher thrusts. Electric thrusters, including resistojets, can present problems related to heat losses, dissociation of the propellant and nozzle erosion. Figure 1 shows the scheme of a propulsion system based on a resistojet.

The nitrous oxide,  $N_2O$ , is a propellant with good potential for use in resistojets, because it can be self-pressurized and can undergo exothermic decomposition. It is non toxic, relatively inert - explodes when it is strongly heated, is compatible with common materials, non-flammable and stable in normal conditions. The  $N_2O$  is gaseous in ambient conditions but, in general, is stored in saturation conditions (52 bar at 20 °C). Some  $N_2O$  properties are shown on Table 1.

Table 1. Properties of nitrous oxide,  $N_2O$ .

Molecular weight	44.013 kg/mol
Boiling point	-88.5°C
Melting point	-90.8°C
Critical temperature	36.4°C
Critical pressure	72.45 bar
Vapour pressure at 20°C	50.8 bar
Conductivity thermal the 0°C	14.57 mW/(m.K)
Density	1.22 g/ml

Source: Air Liquide MSDS Nr:093A\_AI

N<sub>2</sub>O is decomposed when heated above 520 °C. Once initiated the N<sub>2</sub>O decomposition by heating or by a catalyst, it continues in a self-sustained exothermic process attaining an adiabatic decomposition temperature around 1640 °C (Zakirov, 2004). If there is dissociation, it results mainly in the formation of nitrogen and oxygen:



Nitrous oxide can be decomposed by several catalysts using iridium, platinum, rhodium, tungsten carbide, copper, cobalt or gold. Catalysts reduce the initial temperature of decomposition below 520 °C (Lawrence et al, 2000).

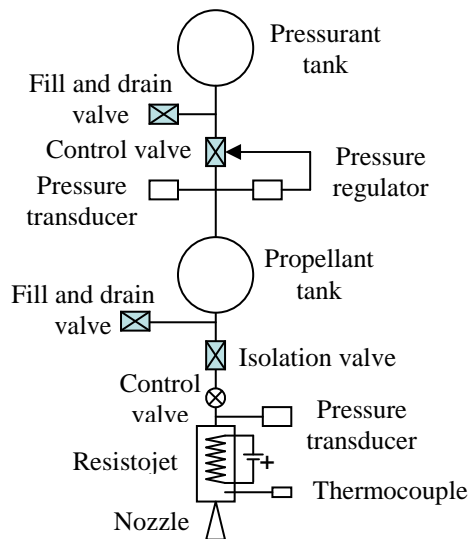


Figure 1. Propulsion system using a resistojet with a pressurization tank.

Table 1 shows a list, presented by Rycek and Zandbergen (2005), of some electrothermal systems launched from 1965 and 1997. It can be seen in Table 1 that the UoSat-12 thruster using nitrous oxide with 100 W power input reached an Isp of 127 s with a thrust of 125 mN.

This paper aims to describe a bench for testing catalytic electrothermal thrusters and the design of a 0.2 N catalytic thruster using self-pressurized nitrous oxide as propellant. Some preliminary results are presented.

Table 1 - Resistojet systems launched from 1965 and 1997.  
 Source: Rycek and Zandbergen (2005).

First launch	Satellite	Propellant	Power [W]	Thrust [mN]	Isp [s]
<b>Application: Experimental</b>					
1967	ATS-2 e ATS-3	Ammonia	3,6	18	150
1968-1969	ATS-4 e ATS-5	Ammonia	3,5	18	150
1971	Sol rad-10	Hydrazine	< 10	-	-
1999	UoSat -12	Nitrous oxide	100	125	127
<b>Application: geosynchronous orbit adjustment</b>					
1980	INTELSAT-V	Hydrazine	300-600	223-490	280
1983	Satcom-1R	Hydrazine	450	178-356	298
1994	GOMS	Ammonia	450	-	-
<b>Application: orbit adjustment</b>					
1965	Vela	Nitrogen	92	187	123
1965	U.S.Navy sat.	Ammonia	30	89	132
1967	Advanced Vela	Nitrogen	30	89	132
1971	U.S.Navy sat.	Ammonia	3	44-356	235
1981	Meteor 3-1	Ammonia	450	-	-
1988	Gstar-3	Hydrazine	600	-	-
1997	Iridium	Hydrazine	500	-	-

## 2. TEST BENCH FOR CATALYTIC RESISTOJETTS

Figures 2 and 3 show, respectively, a scheme and views of an initial version of the test bench. The bench includes a table, support, N<sub>2</sub>O tank, pressure regulator, ducting, valves, flow control system, power source, pressure transducers, thermocouples and data acquisition system. In the initial version of the bench the thruster was near the thrust balance flexures what caused several problems related to heating of the thrust balance. Later it was included an additional support in the bench to reduce errors on thrust measurements caused by heating and dilatation of the thruster.

A pressure regulator is used to reduce the pressure in the N<sub>2</sub>O tank from 52 bar to about 7 bar. The pressure in the heating and catalytic chamber is approximately 5 bar. A filter is used to avoid that propellant impurities block the feed lines. A solenoid valve with an electro-pneumatic valve, remotely controlled, is used to open and shut the flow to the thruster. A check valve is used to avoid flow return and damage to the mass flow controller.

The thruster is supported on a rigid table and a support, as depicted in Figure 3. Other components can also be supported on the table, avoiding vibration, since very low thrusts are being measured. The thruster has a central cartridge heater, a tangential propellant injector and a catalytic bed with a variable length. The thrust is measured by a 3 N load cell, as shown in Fig. 3b. The load cell has a strain gage that sends a voltage signal when it is strained.

The pressure transducers are positioned in the inlet and exit of the catalytic chamber and in the feed line. The thermocouples are placed at the inlet and exit of the catalytic chamber, and inside the resistance, to allow control of the heat input and to provide data to measure the thermal efficiency.

The signals from the pressure transducers and temperature sensors are collected by a data acquisition system with LabView software which also controls the opening and closing of the valves.

In the next section the performance parameters and the detailed design characteristics of an electrothermal catalytic thruster for test are presented.

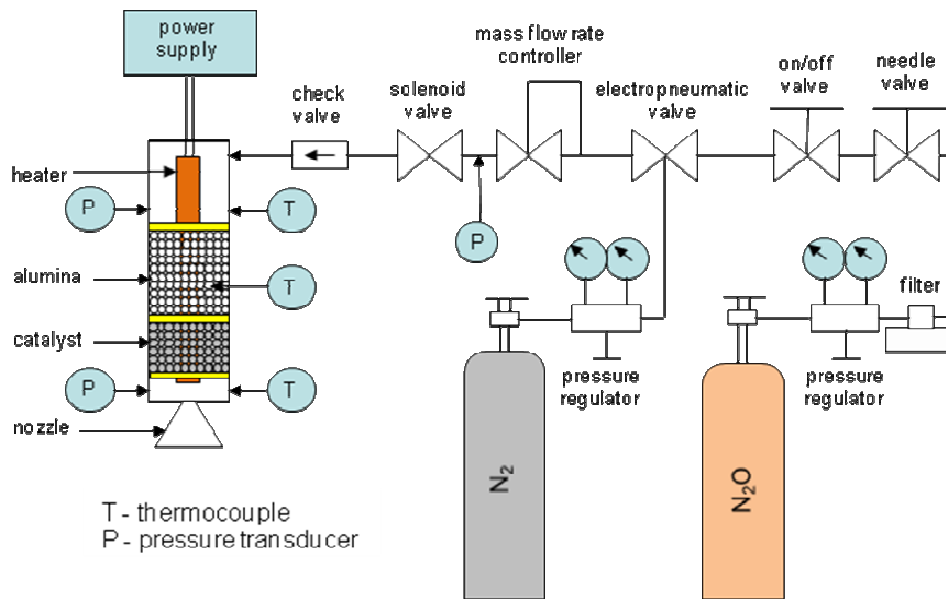
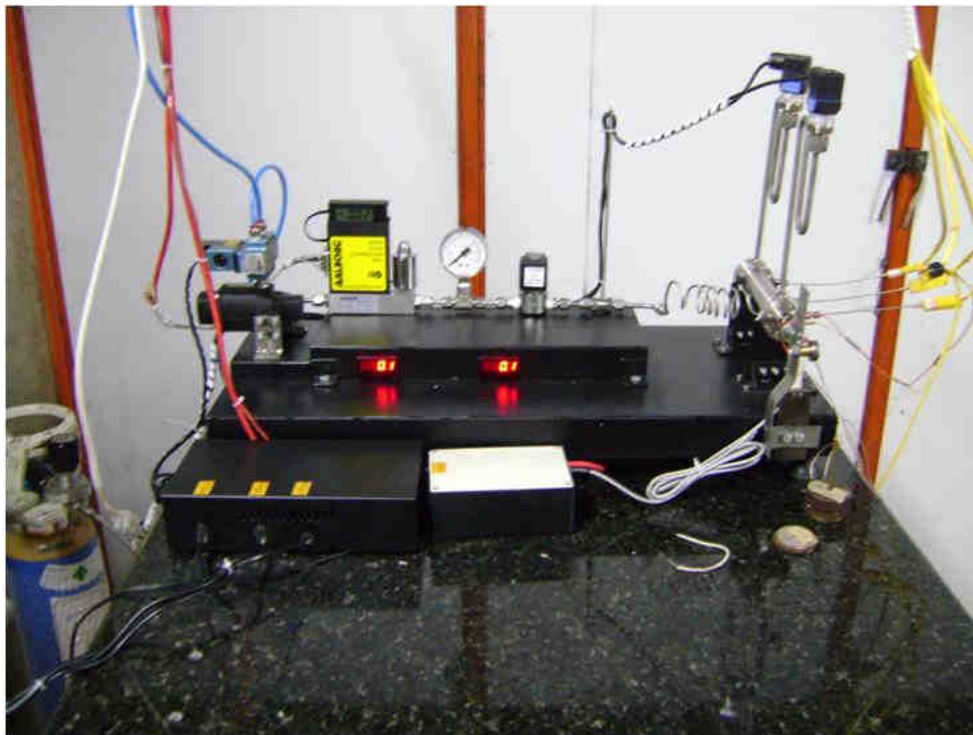


Figure 2. Scheme of test bench with thruster assembled.



a) Bench and thruster during assembling.



b) Bench with assembled thruster under operation.

Figure 3. Early version of the test bench.

### 3. THRUSTER DESIGN

#### 3.1. Performance Parameters

The main performance parameters of a catalytic electrothermal thruster are the maximum chamber temperature, the fraction of decomposed propellant, thrust, thrust coefficient, characteristic velocity, specific impulse and propulsive efficiency. Expressions for some of these parameters were derived previously by Albuquerque and Costa (2008) and are shown next.

The thrust,  $F$ , produced by the ejection of gases in high velocity is given by

$$F = \dot{m}V_e + (p_e - p_a)A_e \quad (1)$$

where  $\dot{m}$  is the mass flow rate of propellant,  $p_e$  is the exhaustion pressure of gases in the nozzle,  $p_a$  is the ambient pressure,  $A_e$  is the exhaustion area of the nozzle and  $V_e$  is the exhaustion velocity of the gases.

The exhaustion velocity is obtained by applying the first law of thermodynamics to the flow in the thruster, yielding,

$$V_e = [2c_{p,e}(T_{oc} - T_e)]^{1/2} \quad (2)$$

where  $T_{oc}$  is the stagnation temperature at the end of the heating/catalytic chamber and  $c_{p,e}$  is the average gas specific heat during exhaustion in the nozzle. The stagnation temperature,  $T_{oc}$ , depends on the dissociation level of the propellant and on the heating efficiency. A study of the propellant dissociation effects was made by Albuquerque and Costa (2008).

The specific impulse,  $I_{sp}$ , is defined by

$$I_{sp} = \frac{F}{\dot{m}g_o} \cong \frac{V_e}{g_o}, \text{ if } P_e \approx P_a, \quad (3)$$

where  $g_o$  is the gravity acceleration at sea level ( $=9.81 \text{ m/s}^2$ ).

The specific impulse,  $I_{sp}$ , is proportional to the exhaustion velocity at the nozzle exit and depends on the chamber pressure, power input, heat losses, friction losses and nozzle expansion ratio.

The thrust coefficient is given by

$$C_F = \frac{F}{P_c A_t} \quad (4)$$

where  $P_c$  is the chamber pressure and  $A_t$  is the nozzle throat area.

$C_F$  indicates the nozzle design quality and does not depend significantly on the propellant choice.

The characteristic velocity,  $C^*$ , indicates the propellant quality and it is given by

$$C^* = \frac{P_c A_t}{\dot{m}} \quad (5)$$

It is defined here the electric propulsive efficiency as the ratio between the power of the exhaustion jet and the power input added to the initial flow enthalpy, yielding

$$\eta_F \cong 1 - \frac{T_e}{T_{oc}} \quad (6)$$

#### 3.2. Design of a Catalytic Resistojet

In order to design an electrothermal catalytic thruster, or catalytic resistojet, several configurations were analysed in the literature. The potential heat losses and the availability of resistances in the Brazilian national market were considered.

Therefore, it was chosen a resistojet configuration including a central heater, i.e., with a cartridge placed along the axis of the heating/catalytic chamber, tangential injector, pre-chamber, alumina and catalytic beds around the heater, post-chamber, thermal insulation and a nozzle.

Figures 4 and 5 show views of the catalytic resistojet designed.

The catalytic bed comprises catalyst grains distributed around the central heater and retained by metal screens. The tangential injector allows a larger contact time between the propellant and the alumina and catalytic bed. Catalysts of iridium or ruthenium impregnated into alumina, manganese oxide and other produced in the LCP/INPE (Combustion and Propulsion Laboratory/Brazilian Space Research Center) can be used for tests.

Table 2 shows reference values adopted, based on a previous thermodynamics analysis (Albuquerque and Costa, 2008) and considering typical values of thrust and electric power available in medium size satellites.

The resistojet comprises, broadly, four sections.

The first section is the pre-chamber which includes the tangential injector and the initial part of the electric resistance. The cold propellant injected cools down the initial part of the resistance which will pass through the other two thruster sections. The resistance is a stainless steel cartridge containing a nickel chrome filament isolated with magnesium oxide.

The second section corresponds to an alumina bed surrounding the resistance and limited by metal screens which retain the alumina grains. Alumina increases the thermal inertia and has potentially a catalytic effect. The gases are injected tangentially, heated in contact with the resistance and, possibly, are decomposed by heating.

The third section includes the catalytic bed and post-heating chamber.

The fourth section comprises the nozzle which converts the thermal energy of the gases into kinetic energy of exhaustion.

Table 2. Reference values for development of a catalytic resistojet.

Maximum power (W)	500
Maximum thrust (N)	0.5
Expansion ratio, $\epsilon$ (-)	4
Throat diameter (mm)	0.94
Thrust coefficient (-)	1.437
Chamber pressure (atm)	5
Maximum specific impulse (s)	200
Mass flow rate (g/s)	0.25

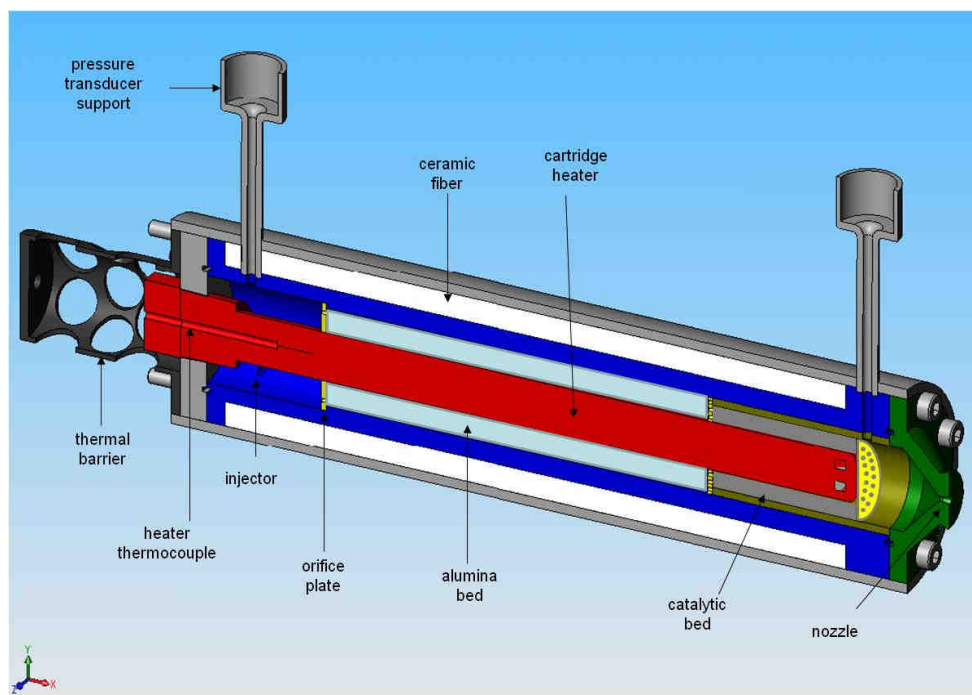
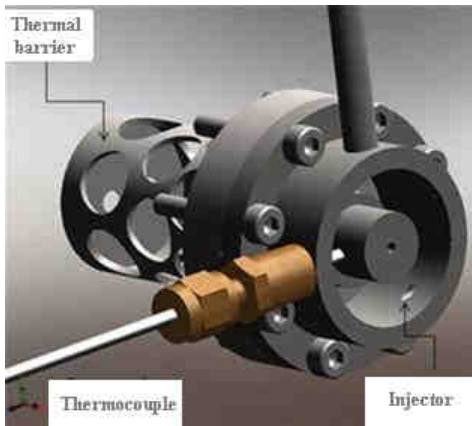
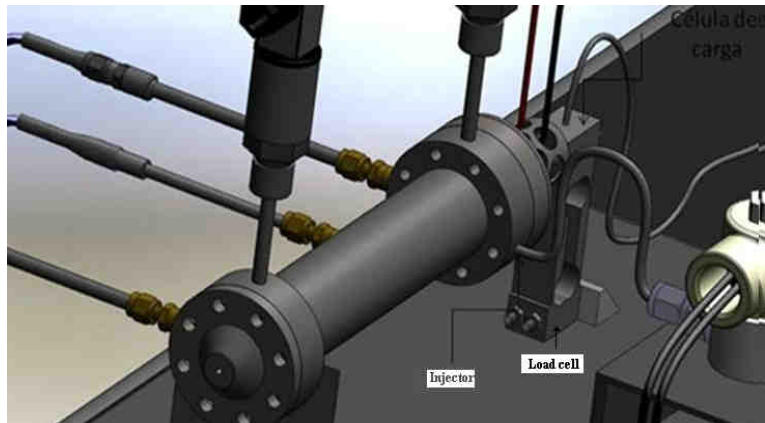


Figure 4. Longitudinal section view of the catalytic resistojet.





a) Pre-chamber cross section.



b) 3D view of the thruster test bench.

Figure 5. 3D views of the bench with the thruster supported on the load cell.

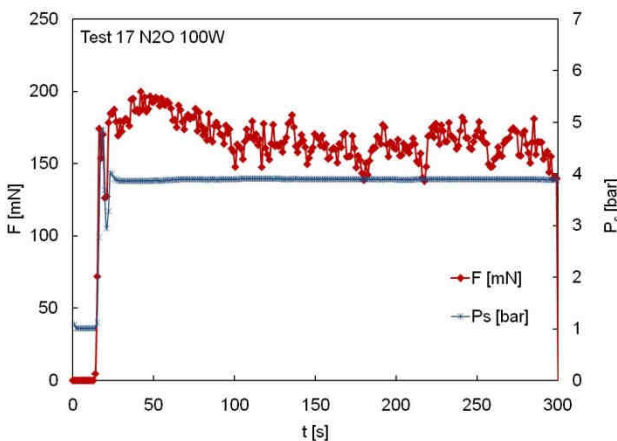
#### 4. EXPERIMENTAL RESULTS

Figure 6 shows the thrust,  $F$ , specific impulse,  $I_{sp}$ , chamber pressure,  $P_s$ , and mass flow rate measured in a test using 75% of the catalytic bed filled with alumina, no catalyst and power input of 100 W. The average specific impulse was around 85 s, average mass flow rate around 0,2 g/s and average thrust about 170 mN.

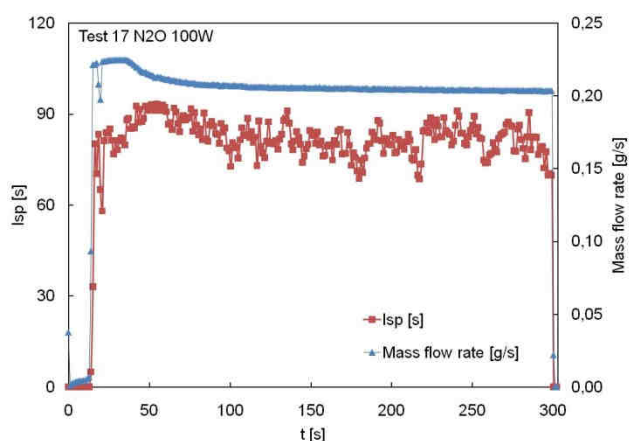
Figures 7 and 8 show results of tests using a ruthenium catalyst supported on alumina ( $Ru/Al_2O_3$ ) with 200 W and 450 W power input, respectively. In these tests 25% of the thermo-catalytic bed were filled with catalysts and 75% were filled with alumina. The heater was turned off as soon as the  $N_2O$  was injected.

The catalytic bed exit temperature,  $T_s$ , increased rapidly after injection of  $N_2O$ , thus indicating that the exothermic decomposition was occurring, since the heater was turned off. The propellant supply was stopped when the electric resistance,  $T_{res}$ , reached about 1100 K, to avoid damage to the heater.

It can be seen in Figures 7a and 8a that the catalytic bed exit temperature ( $T_s$ ) increased up to about 700 K and 850 K, respectively, whereas the alumina bed temperature ( $T_{bed}$ ) was about 490 K and 780 K, respectively, with no significant variation in both cases.



a) Thrust and chamber pressure



b) Specific impulse and mass flow rate

Figure 6. Results for a test using gaseous  $N_2O$ , with no catalyst and a heating input of 100 W.

Figure 9 compares the propulsive efficiencies for the tests shown in Figs. 7 and 8. It appears that the efficiencies follow the catalytic bed exit temperature. The propulsive efficiency was calculated by Eq. 6 assuming  $T_e = T_{amb} = 298$  K and  $T_{oc} = T_s$ . The resistance temperature attained 1100 K in about 130 s in the 200 W test and in about 50 s in the 450 W test.

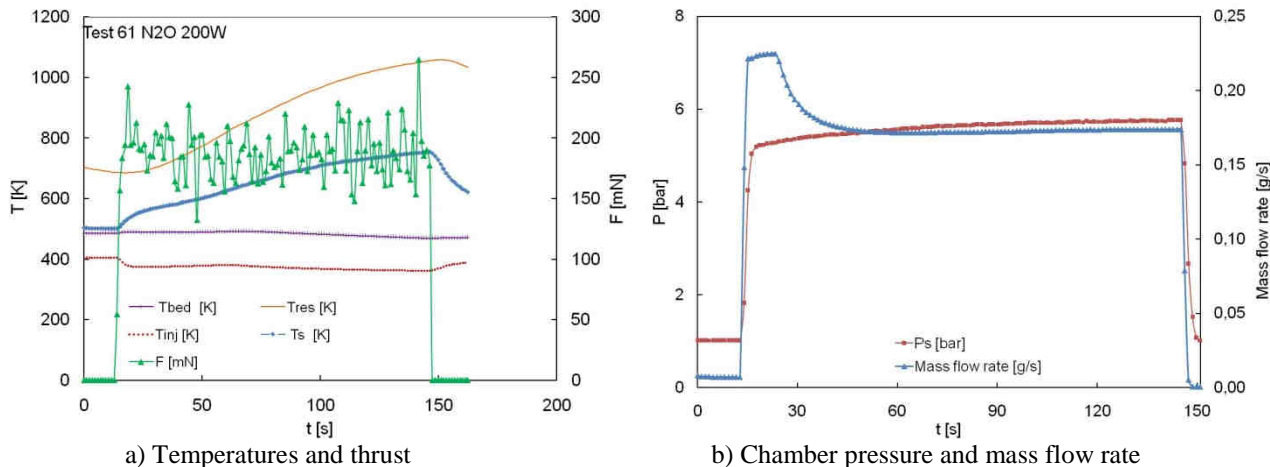


Figure 7. Experimental results for a test using 200W.

Figures 10 and 11 compare test results with catalyst and without catalyst for a power input of 400 W, respectively. Figure 10 shows thrust and chamber pressure whereas Figure 11 shows the mass flow rate and the propulsive efficiency.

Figure 12 shows the effect of power input on thrust and specific impulse in tests with no catalytic decomposition.

In the case without catalyst the thrust did not exceed 100 mN whereas in the case with catalyst the system provided about 200 mN. The increase in thrust is due to the exothermic decomposition of  $N_2O$  which generated a hot mixture of gases with lower molecular weight and a greater exhaust velocity. The chamber pressures were about 4.5 bar in both cases and the mass flow rates without catalysts were smaller than the mass flow rates with catalysts.

The propulsive efficiency for the test with catalyst is higher than for the test without catalyst, in both cases above 50%, due to the large power input.

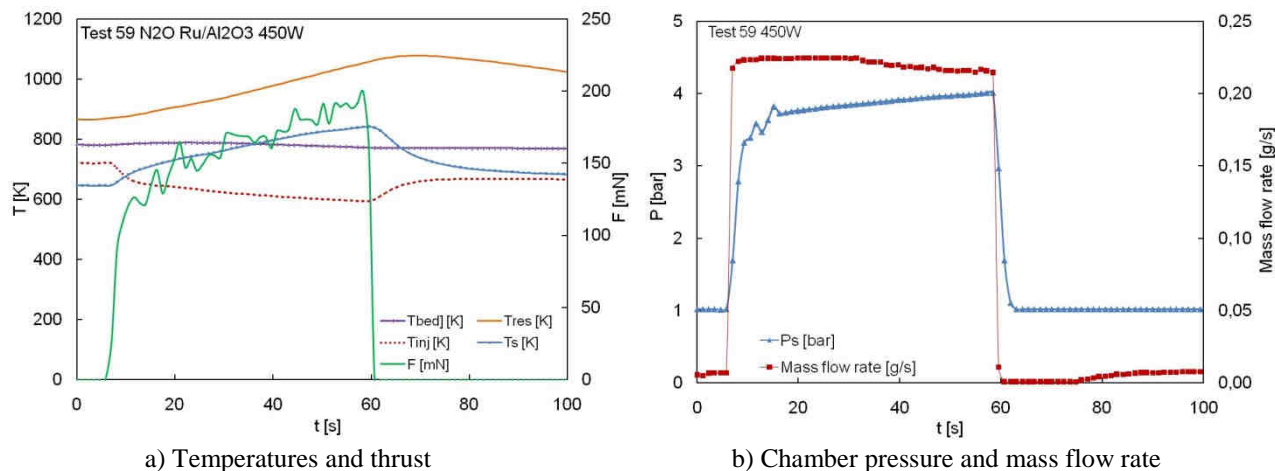


Figure 8. Thruster and temperature profile in the chamber with 450W.

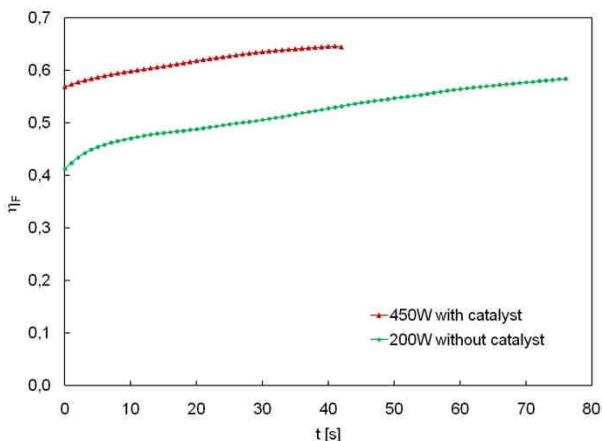
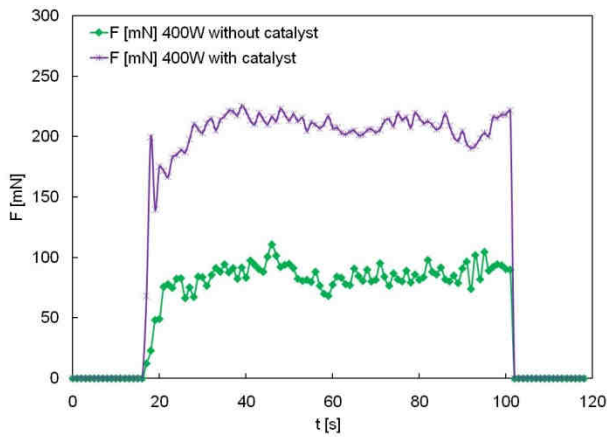
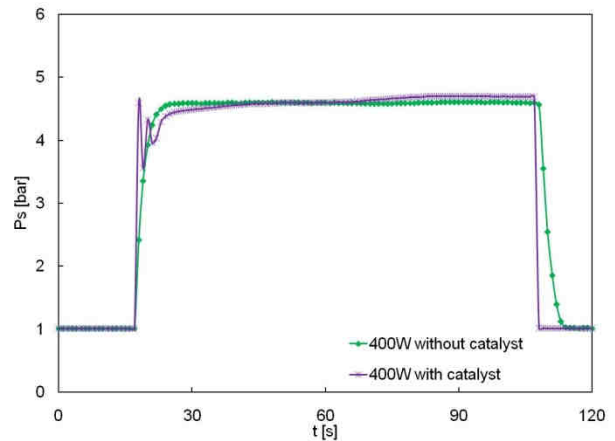


Figure 9. Propulsive efficiency with and without catalyst.



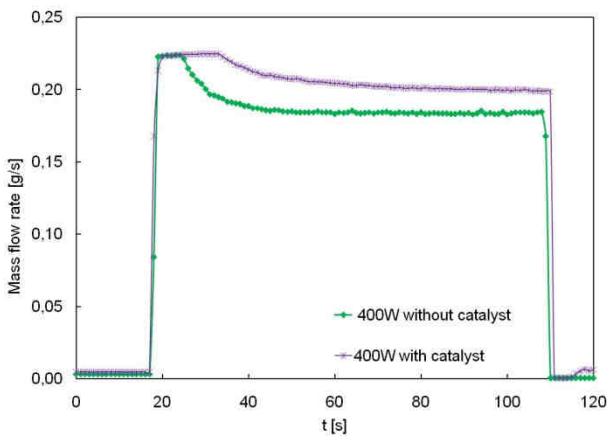


a) Thrust with and without catalyst.

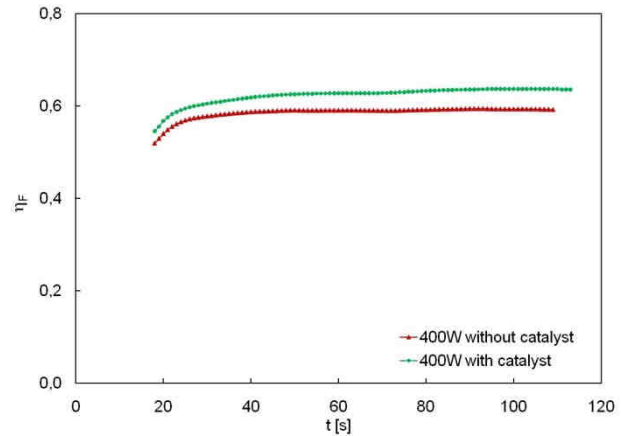


b) Chamber pressure with and without catalyst

Figure 10. Comparison of tests with and without catalyst and 400 W power input.

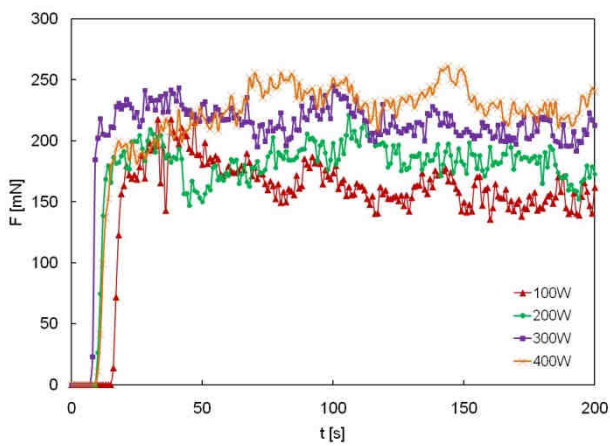


a) Mass flow rate with and without catalyst.

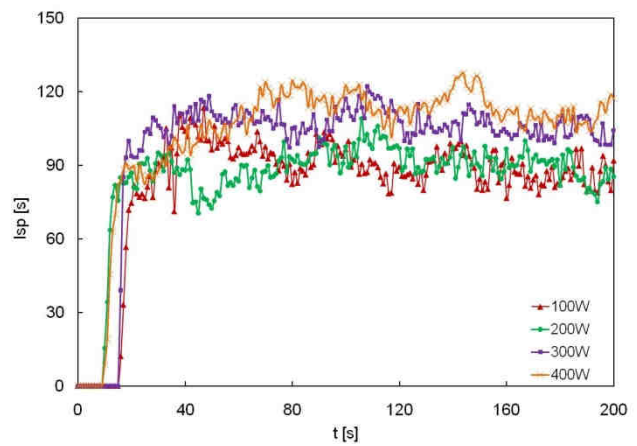


b) Propulsive efficiency with and without catalyst.

Figure 11. Comparison of tests with and without catalyst and 400 W power input.



a) Thrust



b) Specific impulse

Figure 12. Effect of power input on thrust and specific impulse in tests with no catalytic decomposition.

#### 4. CONCLUSION

This work described the design of a bench for testing catalytic resistojets and the design of a 0.2 N catalytic resistojete using self-pressurized nitrous oxide as propellant. Results of preliminary tests in the bench were presented.

Thrust, chamber pressure, temperatures and mass flow rates were measured in different tests with several levels of power input.

Tests with no catalytic decomposition achieved thrust levels 150-250 mN, specific impulses from 70-120 s, and chamber pressures from 4-6 bar.

It was possible to achieve thermo-catalytic decomposition of the nitrous oxide with pre-heating of a Ru/Al<sub>2</sub>O<sub>3</sub> catalyst.

New tests will proceed using different conditions and propellants. Improvements in thruster design, thermal insulation and bench construction are being made.

#### 5. REFERENCES

- Air Liquid S.A., Safety data sheet, 2002, MSDS Nr: 093A\_AL. Page: 1/5. Date: 31/07/2002. <[http://www.aloha.airliquide.com/safety/msds/en/093A\\_AL\\_EN.pdf](http://www.aloha.airliquide.com/safety/msds/en/093A_AL_EN.pdf)>
- Albuquerque-Jr, J., Costa, F.S., Análise Teórica da Performance de um Resistojete Catalítico de Óxido Nitroso, V Congresso Nacional de Engenharia Mecânica, V National Congress of Mechanical Engineering, , Salvador, Bahia, Brasil, 18 a 22 de agosto de 2008.
- Giacobone A., Low thrust propulsion system research (MSc thesis), Delft University of Technology, 2003.
- Hoole R., Resistojete Demonstration Model (in Dutch, MSc thesis). Delft University of Technology, 1990.
- Jahn, R. G., Physics of Electric Propulsion, 1st ed., New York, McGraw-Hill, 1968.
- Lawrence T.J., Zakirov A., Goeman V., Sweeting M. N., "Surrey Research on Nitrous Oxide Catalytic Decomposition for Space Applications". the 14th Annual AIAA/USLJ Conference on Small Satellites. 21-24 August. 2000.
- Rycek, K.; Zandbergen, B. Initial Design of a 1 N Multipropellant Resistojete. In: DUR-1 EUCASS CONFERENCE, 1., 2005, Moscow, Russia, Proceedings, AIAA, 2005.
- Sutton, G.P.; Rocket Propulsion Elements, 7th edition An introduction to the Engineering of rockets. John Wiley and Sons Inc., 1992.
- Szabo J et al., Advances in electrostatic propulsion: ion and Hall thrusters at the Aerospace Corporation, AIAA 95 - 3544, 1995.
- Zakirov V.A., Xueliang, H., Li, L., Prospective N<sub>2</sub>O monopropellant for future small satellite dual-mode propulsion, in: Proceedings of International Symposium on Space Propulsion 2004, Shanghai, China, August 25–28, 2004.

#### 6. RESPONSIBILITY NOTICE

The authors are the only responsible for the printed material included in this paper.